Received: 26 June 2021 | Accepted: 11 September 2021

DOI: 10.1002/prp2.876

ORIGINAL ARTICLE

FJU-C28 inhibits the endotoxin-induced pro-inflammatory cytokines expression via suppressing JNK, p38 MAPK and NF-κB signaling pathways

Fang Jung[1,2] | Jung-Sen Liu[1,3] | Shih-Hsing Yang[1] | Hui-Yun Tseng[1,2,4] | Shang-Shing P. Chou[2] | Jau-Chen Lin[1] | Guey-Mei Jow[5]

[1]Department of Respiratory Therapy, Fu-Jen Catholic University, New Taipei City, Taiwan

[2]Deparment of Chemistry, Fu-Jen Catholic University, New Taipei City, Taiwan

[3]Department of Surgery, Cathay General Hospital, Taipei, Taiwan

[4]Graduate Institute of Biomedical and Pharmaceutical Science, Fu-Jen Catholic University, New Taipei City, Taiwan

[5]School of Medicine, Fu-Jen Catholic University, New Taipei City, Taiwan

Correspondence
Jau-Chen Lin, Department of Respiratory Therapy, Fu-Jen Catholic University, No. 510, Zhongzheng Rd., Xinzhuang Dist., New Taipei City 24205, Taiwan.
Email: 080659@mail.fju.edu.tw

Funding information
This research was supported by grant A0106011 from the Fu-Jen Catholic University, grant 101-CGH-FJU-06 from the Cathay General Hospital, grant 109-2314-B-030-008 from Ministry of Science and Technology.

Abstract

Despite marked improvements in supportive care, the mortality rate of acute respiratory distress syndrome due to the excessive inflammatory response caused by direct or indirect lung injury induced by viral or bacterial infection is still high. In this study, we explored the anti-inflammatory effect of FJU-C28, a new 2-pyridone-based synthetic compound, on lipopolysaccharide (LPS)-induced inflammation in vitro and in vivo models. FJU-C28 suppressed the LPS-induced mRNA and protein expression of iNOS, COX2 and proinflammatory cytokines. The cytokine protein array results showed that LPS stimulation enhanced the secretion of IL-10, IL-6, GCSF, Eotaxin, TNFα, IL-17, IL-1β, Leptin, sTNF RII, and RANTES. Conversely, the LPS-induced secretion of RANTES, TIMP1, IL-6, and IL-10 was dramatically suppressed by FJU-C28. FJU-C28 suppressed the LPS-induced expression of RANTES, but its parental compound FJU-C4 was unable to diminish RANTES in cell culture media or cell lysates. FJU-C28 blocked the secretion of IL-6 and RANTES in LPS-activated macrophages by regulating the activation of JNK, p38 mitogen-activated protein kinase (MAPK) and nuclear factor-κB (NF-κB). FJU-C28 prevented the LPS-induced decreases in lung function including vital capacity (VC), lung compliance (C chord), forced expiratory volume at 100 ms (FEV100), and forced vital capacity (FVC) in mice with LPS-induced systemic inflammatory responses. FJU-C28 also reduced neutrophil infiltration in the interstitium, lung damage and circulating levels of IL-6 and RANTES in mice with systemic inflammation. In conclusion, these findings suggest that FJU-C28 possesses anti-inflammatory activities to prevent endotoxin-induced lung function decrease and lung damages by down-regulating proinflammatory cytokines including IL-6 and RANTES via suppressing the JNK, p38 MAPK and NF-κB signaling pathways.

Abbreviations: ALI, acute lung injury; AMPK, AMP-activated protein kinase; ARDS, acute respiratory distress syndrome; FEV100, forced expiratory volume at 100 ms; FVC, forced vital capacity; H&E, hematoxylin and eosin; IC, inspiratory capacity; LPS, lipopolysaccharide; MAPK, mitogen-activated protein kinase; MTT, 3-(4,5-dimethylthiazol-2-yl)-2,5-diphenyl tetrazolium bromide; NF-κB, nuclear factor-κB; RSV, respiratory syncytial virus; STAT3, signal transducer and activator of transcription 3; VC, vital capacity.

Jau-Chen Lin and Guey-Mei Jow contributed equally to this manuscript.

KEYWORDS
FJU-C28, IL-6, inflammation, lipopolysaccharide, MAPK, NF-κB

1 | INTRODUCTION

Despite marked improvements in supportive care, the mortality rate of acute respiratory distress syndrome (ARDS) due to the excessive inflammatory response caused by viral or bacterial infection-induced direct or indirect lung injury is still high.[1,2] The inflammatory response is an important host defense mechanism that protects against infection and restores damaged tissues to normal physiological states.[3,4] Macrophages play a crucial role in regulating the innate immune response during inflammatory processes.[5] Lipopolysaccharide (LPS) activates macrophages to release various inflammatory mediators and inflammatory cytokines.[6] However, the prolonged production of inflammatory mediators by macrophages can cause an inflammatory response, eliciting the release of various vascular and cellular danger signals that promote damage to the host and contribute to the pathology of many inflammatory diseases.[7] Therefore, developing effective agents is important for creating new therapeutic approaches for the treatment of inflammatory diseases.

IL-6 is a major proinflammatory mediator that induces the acute-phase response, severe asthma and inflammatory pulmonary diseases.[8–10] IL-6 is a major activator of signal transducer and activator of transcription 3 (STAT3) and blocks apoptosis in cells during the inflammatory process, keeping these cells alive in toxic environments.[11] Several lines of evidence suggest that IL-6 is a pleiotropic cytokine during the transition from innate to acquired immunity to prevent increased tissue damage from the accumulation of neutrophil-secreted proteases and reactive oxygen species during inflammation.[11,12] Studies have demonstrated that several signaling pathways, including the nuclear factor-κB (NF-κB) and mitogen-activated protein kinase (MAPK) signaling pathways, are upregulated in animal models of acute lung injury (ALI).[13–16] NF-κB plays a pivotal role in immune and inflammatory responses through the regulation of proinflammatory cytokines, adhesion molecules, chemokines, growth factors and inducible enzymes.[17] Recently, reports have shown that p38 MAPK contributes to LPS-induced IL-6 secretion.[18] Studies have shown that stimulating both the p38 MAPK and NF-κB signaling pathways can induce IL-6 gene expression and release.[19]

RANTES (also called CCL5) is a C-C chemokine that plays an important role in recruiting leukocytes, including T lymphocytes, macrophages, eosinophils, and basophils, to inflammatory sites.[20] Several infectious diseases caused by viruses, including dengue viruses, respiratory syncytial virus (RSV) and influenza virus A, cause airway inflammation and significantly induce RANTES secretion and expression in humans and animal models.[21–24] Recent studies have demonstrated that SARS coronavirus (SARS-CoV) and RSV infection can induce high levels of IL-6 and RANTES (CCL5) in a cell model.[25] High expression of RANTES after primary respiratory syncytial viral infection is associated with the exacerbation of airway disease; RSV-infected animals treated with anti-RANTES antibodies showed significant decreases in airway hyperreactivity.[26] RANTES expression is associated with CD45-positive inflammatory cell infiltration, which causes pulmonary arterial hypertension.[27] Several animal models of ARDS have shown elevated expression of RANTES induced by either LPS or caerulein, which lead to systemic inflammatory responses and distant lung injury.[28,29] The treatment of caerulein-induced pancreatitis in mice with Met-RANTES can reduce lung damage.[30] In addition, blocking the RANTES receptor CC-chemokine receptor type 5 may reduce and prevent lung damage in complement component 5a-induced ALI.[31] This evidence suggests that RANTES is involved in various physiopathological processes and may be a target for a new therapeutic strategy by interfering with the binding of this chemokine to its proteoglycan receptor. However, the exact functions of RANTES in pathogen-induced inflammation are still unclear.

2-Pyridones are a class of potent antibacterial agents that are used to treat bacterial infections caused by gram-negative bacteria; these agents are effective treatments that targets the early release of proinflammatory cytokines and are useful for preventing and/or treating inflammation related to leukocyte infiltration.[32] FJU-C28, which is derived from a 2-pyridone compound,[13] was recently synthesized, and its anti-inflammatory activities and underlying mechanisms remain unknown. In this study, the anti-inflammatory effects of FJU-C28 on the expression of inflammatory mediators were analyzed in vitro, and the efficacy of FJU-C28 in improving lung function in ALI was evaluated by using an in vivo animal model. The profile of cytokines in macrophages with LPS-induced inflammation was identified by using a cytokine protein array, and then the molecular mechanism of the dominant cytokines, including IL-6 and RANTES, in the progression to ARDS was manipulated by using in vitro cell models.

2 | MATERIALS AND METHODS

2.1 | Cell culture

RAW264.7 cells (mouse monocyte/macrophage-like cells) were purchased from the Bioresource Collection and Research Center (Hsinchu, Taiwan). The cells were maintained in DMEM (HyClone) containing 10% fetal bovine serum (HyClone), MEM nonessential amino acids (HyClone), 100 mM sodium pyruvate (HyClone), and penicillin/streptomycin (HyClone). The cells were incubated at 37°C in a humidified atmosphere of 5% CO_2 and 95% air.

2.2 | Chemicals

The FJU-Cs compound used in this study was synthesized at the Department of Chemistry at Fu-Jen Catholic University, Taiwan. LPS (*Escherichia coli* 0111:B4; Catalogue Number: L4391) was purchased

from Sigma-Aldrich. BAY11-7082 (NF-κB inhibitor), PD98059 (ERK1/2 inhibitor), SB203580 (p38 MAPK inhibitor) and SP600125 (JNK inhibitor) were purchased from Enzo Life Sciences. Rapamycin (mTOR inhibitor) and Wortmannin (Phosphatidylinositol 3-kinase Inhibitor) was purchased from Abcam Biotechnology. CLI-095 (TLR4 signaling inhibitor) was purchased from InvivoGen.

2.3 | Cytokine protein array analysis

Cytokine array analysis was performed according to the procedure recommended by the Raybio mouse cytokine antibody array 4 (RayBiotech, Inc.). This cytokine protein array was used to simultaneously determine the relative levels of 40 different cytokines, chemokines, and acute-phase proteins in a single sample. One hundred microliters of cell culture medium was used for each sample. The signal intensity in the membrane of the cytokine protein array was measured by using ImageJ software and is presented as a heat map drawn by using MultiExperiment Viewer (MeV V.4.9.0) software.

2.4 | Quantitative real-time PCR

RNA was isolated from cells using TRIzol reagent (Invitrogen) as previously described.[32] The concentration of the isolated RNA was measured using an Epoch microplate spectrophotometer (BioTek). One microgram of RNA was reverse-transcribed to cDNA with random primers and an MMLV RT kit (Epicenter Biotechnologies). The mixture (2 μl) was added to PCR reagents to measure the target mRNA level with specific primers (Table 1). All real-time PCRs were performed in a volume of 20 μl containing 10 μl of Real-time PCR SYBR Green master mix (Toyobo) using a PikoReal 96 Real-Time PCR System (Thermo Fisher Scientific Inc.), according to our previously described method.[33] The expression of β-actin was used as an internal control for RNA quantification.

2.5 | Enzyme-linked immunosorbent assay

RANTES (RayBiotech), IL-1β and IL-6 (eBioscience) concentrations in cell culture media and mouse serum were measured using Enzyme-linked immunosorbent assay (ELISA) kits according to the manufacturer's instructions. The plates were measured at 450 nmol/L using an Epoch microplate spectrophotometer (BioTek Instruments). The concentrations of RANTES, IL-1β and IL-6 in the samples were determined by standard curves.

2.6 | Western blotting

In brief, cell lysate was separated by 10% SDS–PAGE and transferred to a PVDF membrane (HybondTM-P; Amersham). The blots were probed with anti-p38 MAPK (Catalogue Number: 8690P), anti-p-p38 MAPK (Thr180/Tyr182; Catalogue Number: 4511P), anti-ERK44/42 (Catalogue Number: 4695P), anti-p-ERK44/42 (Thr202/Tyr204; Catalogue Number:4370P), anti-JNK (Catalogue Number: 9258P), anti-p-JNK (Thr183/Tyr185; Catalogue Number: 4668P), anti-p65 (Catalogue Number: 8242S), anti-STAT3 (Catalogue Number: 12640S), anti-p-STAT3 (Tyr705; Catalogue Number: 9145S) and anti-RANTES (Catalogue Number: 2989S) antibodies were provided by Cell Signaling Technology, Inc.. Anti-Lamin A/C (Catalogue Number: 101127) antibodies were obtained from GeneTex, Inc.. Anti-β-Actin (Catalogue Number: SC-47778) and anti-COX2 (Catalogue Number: SC-1746) antibody was obtained from Santa Cruz Biotechnology, Inc.. The anti-iNOS (Catalog Number: 610329) antibody was obtained from BD transduction Lab.. Bound antibodies were visualized by electrochemical luminescence staining (Western Lighting Plus ECL; PerkinElmer) with autoradiography using FUJI Medical X-ray film (Fuji Corporation) or a MultiGel-21 multifunctional imaging system (TOPBIO). The intensity of the western blot bands was quantified by ImageJ software. The quantitative immunoblot data were normalized to the internal control protein and are expressed as the relative ratio of the treatment group to the control. The data represent the mean ± *SD*. of at least three independent experiments.

2.7 | Analysis of cell viability

RAW264.7 macrophages were pretreated with FJU-Cs (0 to 10 μM) as indicated for 30 min and were then stimulated with/without LPS (100 ng/ml) for 24 h. The remaining cells were evaluated by a 3-(4,5-dimethylthiazol-2-yl)-2,5-diphenyl tetrazolium bromide (MTT) assay. Cells containing formazan crystals were dissolved in DMSO (Merck) and quantified at a wavelength of 595 nm using a spectrophotometer

TABLE 1 Real-time PCR primers

Gene	Forward primer (5′)	Reverse primer (3′)	Size (bp)
iNOS	GAAGAAAACCCCTTGTGCTG	GTCGATGTCACATGCAGCTT	138
COX2	GATGTTTGCATTCTTTGCCC	GGCGCAGTTTATGTTGTCTG	149
IL-1β	CGCAGCAGCACATCAACAAGAGC	TGTCCTCATCCTGGAAGGTCCACG	111
IL-6	CACAAGTCCGGAGAGGAGAC	CAGAATTGCCATTGCACAAC	141
β-actin	GATTACTGCTCTGGCTCCTAGC	GACTCATCGTACTCCTGCTTGC	147

(BioTek Instruments, Inc.). Each experiment was repeated at least three times.

2.8 | Animal model

Ten-week-old male C57BL/6 mice from BioLasco Taiwan Co., Ltd. were used in the present study. The mice were maintained under standard laboratory conditions as described in a previous study.[34] All animal procedures were approved by the Institutional Animal Care and Use Committee of Fu Jen Catholic University (IACUC approval number: A10508). We also confirmed that all experiments were performed in compliance with the ARRIVE guidelines. All surgeries were performed under anesthesia, and all efforts were made to minimize the pain and discomfort of the animals. The mice were randomly assigned to three groups: control ($n = 7$), LPS ($n = 7$) and LPS plus C28 ($n = 8$). The mice were injected with/without FJU-C28 (5 mg/kg) dissolved in DMSO/PBS buffer, and after 1 h the mice were stimulated with an intraperitoneal injection of LPS (7.5 mg/kg) in PBS buffer. At 24 h after LPS stimulation, the mice were anesthetized i.p. with a mixture of ketamine (100 mg/kg) (Pfizer) and xylazine (10 mg/kg) (Bayer), endotracheally intubated with an airway catheter and connected to a forced pulmonary maneuver system (Buxco Research System; Buxco Electronics). The detailed procedure was performed as described in a previous study.[34] The lung function values, including C chord (lung compliance), IC (inspiratory capacity), VC (vital capacity), FEV100 (forced expiratory volume at 100 ms) and FVC (forced vital capacity), were measured using a Buxco Research System. After the lung function assays, the experimental mice were sacrificed, and blood was collected by cardiac puncture. The lung lobes were inflated with 4% buffered paraformaldehyde via a catheter. Slides of lung specimens at a thickness of 5 μm were stained with hematoxylin and eosin (H&E) for light microscopic analysis.

2.9 | Statistical analysis

The data for triplicate experiments are expressed as the means and standard errors. All statistical analyses were performed by one-way ANOVA, followed by Tukey's multiple comparison post hoc test. A value of $p < .05$ was considered to be significant.

3 | RESULTS

3.1 | Effect of FJU-C28 on the activation of LPS-induced RAW264.7 macrophages

To compare the anti-inflammatory effects of the newly synthesized compound FJU-C28 (Figure 1A) on LPS-activated murine macrophages to those of the parent compound FJU-C4,[13] RAW264.7 macrophages were pretreated with various concentrations of FJU-Cs for 30 min and then stimulated with or without LPS for 24 h. FJU-C28 protected RAW264.7 macrophages from LPS-induced cell death and exhibited less cytotoxicity than 10 μM FJU-C4 (Figure 1B). LPS stimulation changed the shape of macrophages, resulting in dendritic-like cells with multiple vacuoles in the cytoplasm, whereas the untreated cells were round and small. FJU-C28 dramatically inhibited these changes in morphology in a concentration-dependent manner, and the morphology was similar to that of untreated cells (Figure 1C). This effect was consistent with the findings of the cytotoxicity assay. This result indicated that FJU-C28 could suppress the inflammatory response induced by LPS in RAW264.7 macrophages. In addition, FJU-C28 suppressed the expression of iNOS and COX2 at doses higher than 5 μM (Figure 1D). The quantitative immunoblot data are shown in Figure 1E.

3.2 | Inhibitory effects of FJU-C28 on the transcriptional regulation of inflammatory mediators and proinflammatory cytokines

The effects of FJU-C28 on the gene expression of proinflammatory cytokines and late inflammatory mediators in macrophages were analyzed by using quantitative real-time RT-PCR (Figure 2). The results showed that the mRNA levels of iNOS and COX2 were downregulated in a concentration-dependent manner. The mRNA levels of the proinflammatory cytokine IL-6 and IL-1β were concentration-dependently decreased when the concentration of FJU-C28 was less than 10 μM. FJU-C28 noticeably inhibited the gene expression of IL-6 and iNOS when the dose was higher than 5 μM. These results indicated that FJU-C28 significantly reduced the transcription of the proinflammatory cytokine including IL-6 and IL-1β in LPS-induced RAW264.7 macrophages.

3.3 | Cytokine expression profile in various conditioned media

To distinguish the effect of various FJU-Cs on LPS-induced inflammation, the cell culture media of RAW264.7 macrophages treated with various conditions were harvested and analyzed by using a mouse cytokine antibody array (left panel of Figure 3). The signal intensities on the array membranes were quantified by densitometry, and the changes in different cytokines are represented as a heat map (right panel of Figure 3). The results showed that several cytokines, including IL-10, IL-6, GCSF, eotaxin, TNFα, IL-17, IL-1β, leptin, sTNF RII, and RANTES, were enhanced by LPS stimulation by at least 5-fold compared to those in the culture media of untreated cells. Moreover, the secretion of the RANTES, TIMP1, IL-6 and IL-10 cytokines was dramatically suppressed by FJU-C28 treatment. Although LPS-induced secretion of TIMP1, IL-6 and IL-10 was also suppressed by FJU-C4 treatment, the expression of RANTES was not changed by FJU-C4 treatment (Table 2).

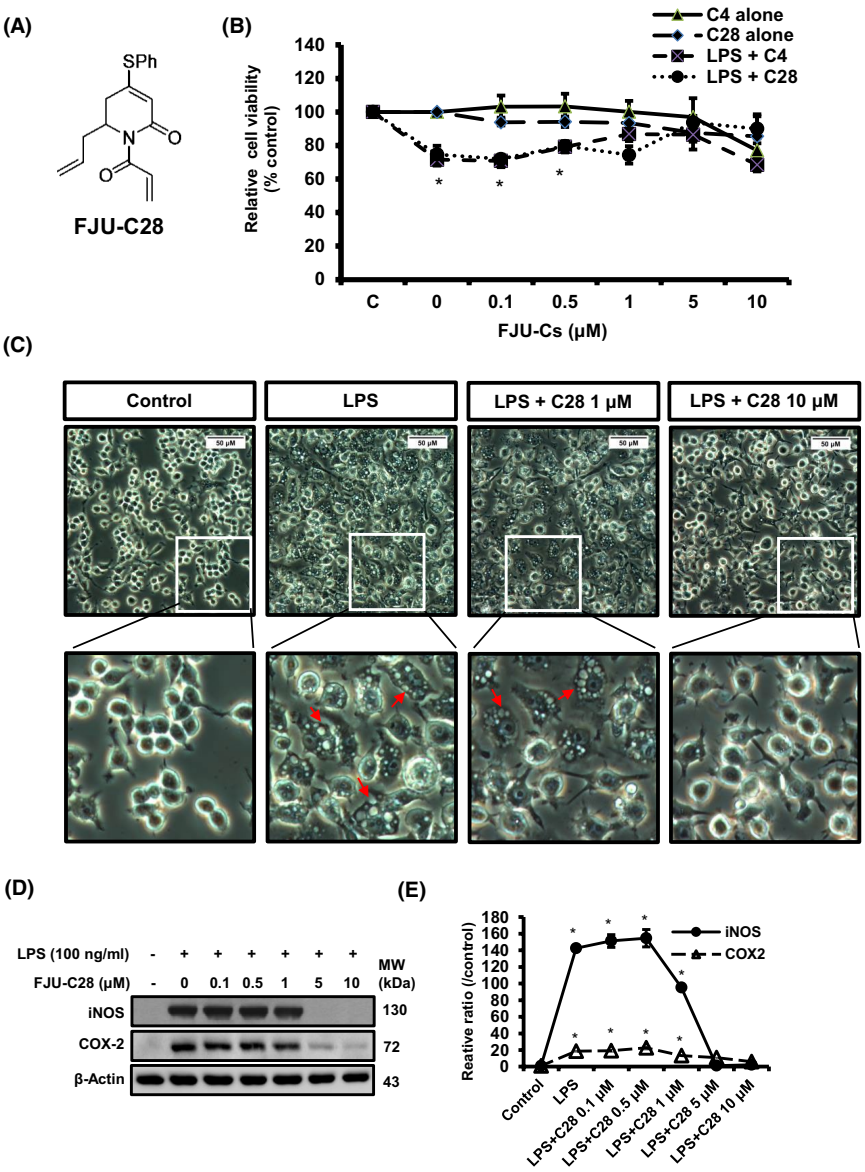

FIGURE 1 Effect of FJU-C28 on the activation of LPS-induced RAW264.7 macrophages. (A) Chemical structure of FJU-C28. (B) Viability of macrophages exposed to FJU-Cs alone or in combination with LPS was measured by MTT assays. (C) Morphological changes in various treated cells were observed by microscopy (400×). LPS-stimulated macrophages resulted in dendritic-like cells with multiple vacuoles in the cytoplasm as indicated by red arrow. Bar = 50 μm at 400× magnification as indicated. Control cells were not treated with LPS. (D) Western bot analysis of iNOS and COX2. β-Actin was used as a loading control. (E) The quantitative immunoblot data were normalized to the internal control protein and are expressed as the relative ratio of the treatment group to the control. The data represent the mean ± *SE* ($N = 3$). $^{*}p < .05$, compared with the control group. LPS, lipopolysaccharide; MTT, 3-(4,5-dimethylthiazol-2-yl)-2,5-diphenyl tetrazolium bromide

3.4 | FJU-C28 suppressed the LPS-induced expression of RANTES and IL-6

To confirm whether FJU-C28 can suppress the expression of RANTES in RAW264.7 macrophages, the cell culture media and cell lysates of RAW264.7 macrophages treated with various conditions were harvested for ELISA and western blot analysis. The ELISA results showed that the expression of RANTES was enhanced in cell culture media and cell lysates of LPS-treated cells; FJU-C28 dramatically suppressed the LPS-induced expression of RANTES, but FJU-C4 was unable to reduce the LPS-induced expression of RANTES at 6 h or 24 h (Figure 4A). In addition, western blot analysis also confirmed that FJU-C28 dramatically suppressed the LPS-induced protein expression of RANTES at 6 h, but FJU-C4 did not reduce the protein expression of RANTES in treated cells (Figure 4B). The secretion of proinflammatory cytokines such as IL-6 and IL-1β in cell culture media was also analyzed by ELISA (Figure 4C,D). The results showed that FJU-C28 dramatically reduced the production of RANTES, IL-6 and IL-1β in LPS-treated macrophages.

3.5 | Effects of FJU-C28 on LPS-induced MAP kinase phosphorylation and NF-κB translocation

For identifying the potential signaling pathways which regulate the secretion of IL-6 and RANTES induced by LPS stimulation, RAW264.7 macrophages were pretreated with various kinase inhibitors for 30 min and then stimulated with/without 100 ng/ml LPS for 24 h; the cell culture media was harvested for ELISA assay. The results showed that LPS-induced expression of IL-6 and RANTES were suppressed by CLI-095 (TLR4 inhibitor), BAY11-7082 (IkB-α Inhibitor), SB203580 (p38 MAPK inhibitor) and SP600125 (JNK inhibitor), but not by PD98059 (ERK inhibitor), Rapamycin (mTOR inhibitor) and Wortmannin (Phosphatidylinositol 3-kinase Inhibitor) (Figure 5A,B). It indicated that LPS stimulate TLR4 signaling to induce

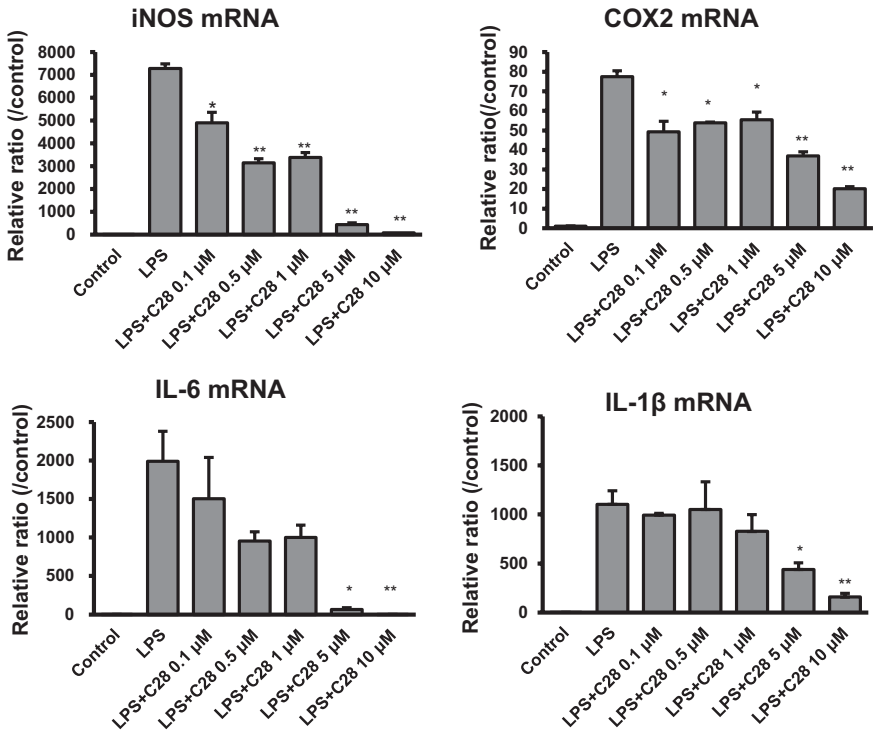

FIGURE 2 Inhibitory effects of FJU-C28 on the LPS-induced transcription of proinflammatory cytokines and inflammatory mediators. Quantitative RT-PCR was performed with the specific primers listed in Table 1. The expression of β-actin was used as an internal control for quantity. The data represent the mean ± *SE* ($N = 3$) (*$p < .05$ or **$p < .01$ vs. the LPS treatment group). LPS, lipopolysaccharide

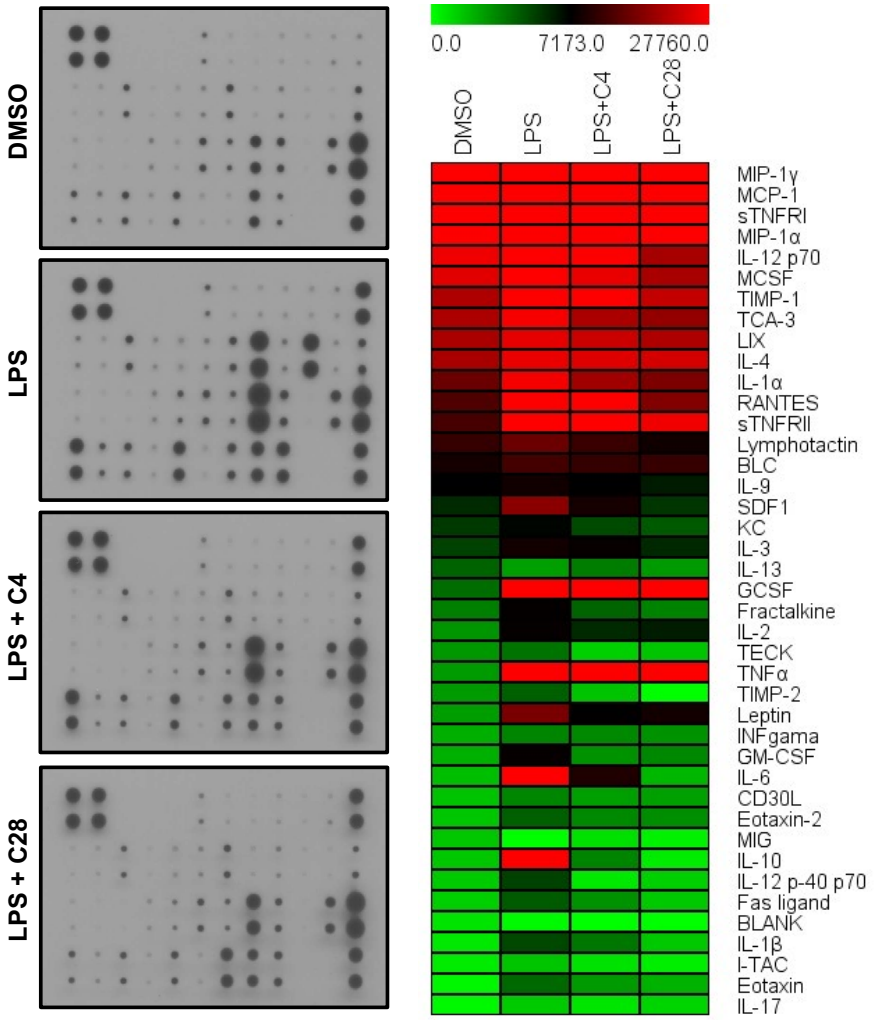

FIGURE 3 Array data of the expression profiles of cytokines in conditioned culture media from RAW264.7 macrophages treated with various compounds. RAW264.7 macrophages were pretreated with FJU-C4 (10 μM) or FJU-C28 (10 μM) for 30 min and then stimulated with/without 100 ng/ml LPS for 24 h. The cell culture media were harvested for cytokine antibody array analysis. (Left panel) A mouse cytokine antibody array was used to analyze the different conditioned media as indicated. (Right panel) The signal intensities on the array membranes were quantified by densitometry, and the changes in different cytokines are shown as a heat map in the right panel. The signals ranged from 0 to 27760. The green and red colors represent low and high expression, respectively. LPS, lipopolysaccharide

TABLE 2 Protein array analysis

Symbol	Control	Protein array, fold change (mean ± *SE*)		
		LPS/control	LPS + C4/control	LPS + C28/control
IL-10	1.0	63.6 ± 1.7	2.2 ± 0.6	0.3 ± 0.2
IL-6	1.0	53.9 ± 2.9	5.5 ± 0.0	1.1 ± 0.2
GCSF	1.0	22.3 ± 0.7	18.8 ± 1.0	20.1 ± 1.9
Eotaxin	1.0	20.3 ± 0.1	13.5 ± 2.9	10.3 ± 6.1
TNFα	1.0	12.3 ± 1.0	11.8 ± 0.9	21.0 ± 0.8
IL-17	1.0	9.8 ± 1.3	4.6 ± 0.8	7.8 ± 5.3
IL-1β	1.0	8.5 ± 0.4	6.3 ± 0.2	2.6 ± 0.0
Leptin	1.0	6.3 ± 0.9	2.7 ± 0.2	3.2 ± 0.8
sTNFRII	1.0	5.4 ± 0.3	2.2 ± 0.1	2.1 ± 0.1
RANTES	1.0	5.2 ± 0.4	5.0 ± 0.5	1.3 ± 0.2
IL-12 p-40 p70	1.0	3.7 ± 0.9	0.4 ± 0.9	0.9 ± 0.1
GM-CSF	1.0	3.5 ± 0.3	1.4 ± 0.0	1.5 ± 0.4
Fas ligand	1.0	3.5 ± 0.1	2.3 ± 0.9	1.1 ± 0.8
I-TAC	1.0	3.1 ± 0.6	1.5 ± 0.2	0.8 ± 0.3
SDF1	1.0	3.1 ± 0.2	1.5 ± 0.3	0.9 ± 0.2
Eotaxin-2	1.0	2.8 ± 0.3	2.1 ± 0.1	2.0 ± 1.0
TIMP-1	1.0	2.8 ± 0.2	1.9 ± 0.2	1.1 ± 0.1
MCP-1	1.0	2.7 ± 0.1	2.5 ± 0.2	1.7 ± 0.2
IL-2	1.0	2.6 ± 0.1	2.0 ± 0.1	2.1 ± 0.2
Fractalkine	1.0	2.1 ± 0.1	1.2 ± 0.2	1.0 ± 0.6
CD30 L	1.0	2.0 ± 0.4	1.6 ± 0.1	1.6 ± 0.9
IL-1α	1.0	1.7 ± 0.1	1.3 ± 0.1	1.1 ± 0.1
IL-3	1.0	1.7 ± 0.1	1.5 ± 0.1	1.1 ± 0.2
TIMP-2	1.0	1.6 ± 0.4	0.6 ± 0.0	0.0 ± 0.0
INF gamma	1.0	1.6 ± 0.2	1.5 ± 0.2	1.4 ± 0.2
sTNFRI	1.0	1.5 ± 0.1	1.1 ± 0.1	1.0 ± 0.0
BLC	1.0	1.4 ± 0.1	1.3 ± 0.1	1.3 ± 0.1
Lymphotactin	1.0	1.4 ± 0.1	1.0 ± 0.0	0.7 ± 0.2
MCSF	1.0	1.4 ± 0.1	1.0 ± 0.2	0.8 ± 0.1
TECK	1.0	1.3 ± 0.2	0.5 ± 0.3	0.5 ± 0.3
MIP-1α	1.0	1.3 ± 0.1	1.2 ± 0.1	1.0 ± 0.2
TCA-3	1.0	1.3 ± 0.1	1.0 ± 0.1	0.9 ± 0.1
KC	1.0	1.3 ± 0.0	0.9 ± 0.0	0.8 ± 0.4
IL-4	1.0	1.3 ± 0.0	1.2 ± 0.1	1.2 ± 0.2
IL-12 p70	1.0	1.2 ± 0.1	1.0 ± 0.1	0.8 ± 0.2
LIX	1.0	1.2 ± 0.1	1.1 ± 0.1	1.0 ± 0.2
IL-9	1.0	1.2 ± 0.2	1.0 ± 0.2	0.9 ± 0.3
MIP-1γ	1.0	1.0 ± 0.0	1.0 ± 0.0	1.2 ± 0.2
IL-13	1.0	0.6 ± 0.0	0.8 ± 0.0	0.6 ± 0.0

Note: Abbreviation: LPS, lipopolysaccharide.

the expression of IL-6 and RANTES through activation of NF-kB, p38 MAPK and JNK signaling pathways but not ERK, PI3K or mTOR signaling pathways. We further investigated the potential inhibitory effect of FJU-C28 on the activation of MAPKs in LPS-stimulated macrophages. Treatment with 5 and 10 μM FJU-C28 dramatically inhibited LPS-induced levels of p-ERK, p-p38 and p-JNK MAP kinase in macrophages (Figure 6A). The quantitative immunoblot data are shown in Figure 6B. To investigate whether FJU-C28 could mediate the transcriptional activity of NF-κB (p65), the translocation of NF-κB p65 was examined in LPS-stimulated macrophages. The

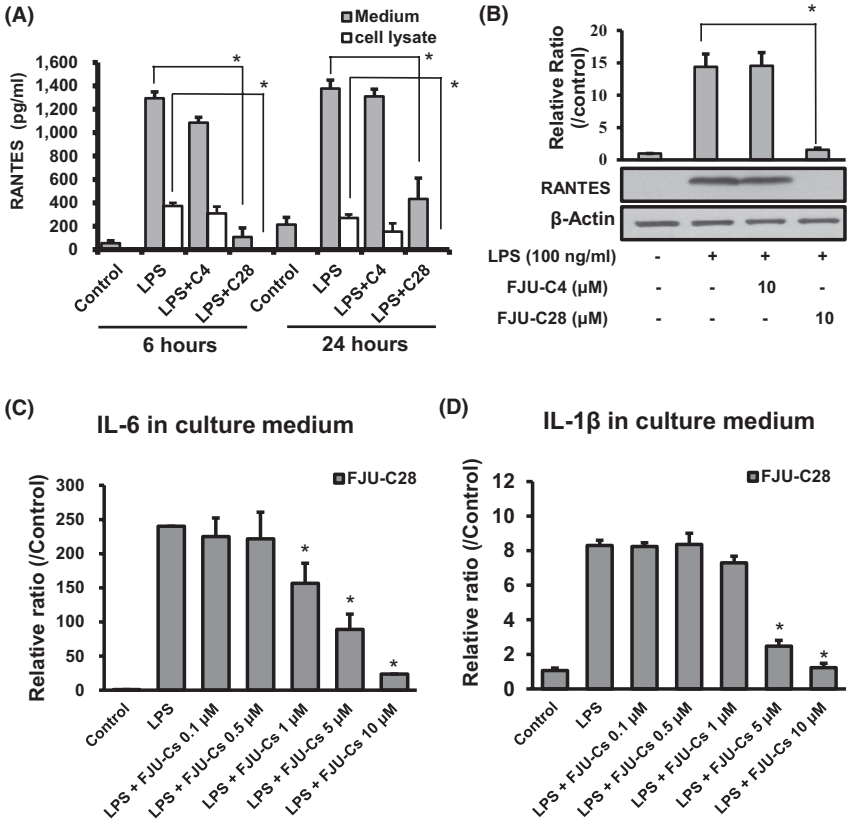

FIGURE 4 FJU-C28 suppressed the LPS-induced expression of cytokines in RAW264.7 macrophages. (A) The level of secreted RANTES in conditioned media. RAW264.7 macrophages were pretreated with 10 μM FJU-C4 or FJU-C28 for 30 min and then stimulated with LPS (100 ng/ml) for 6 h or 24 h. The conditioned media of cells treated with LPS for 6 h or 24 h were harvested and analyzed by ELISA. (B) Cells treated with LPS for 6 h were harvested and analyzed by western blotting with a specific antibody. The quantitative immunoblot data are shown in the upper panel. (C) The level of secreted IL-6 and (D) IL-1β in the conditioned media of cells treated with LPS for 24 h was also analyzed by ELISA. The quantitative data are expressed as the mean ± *SE* ($n = 6$) $^*p < .05$ compared with LPS treatment. LPS, lipopolysaccharide

results showed that the level of NF-κB p65 in the nuclear extract was markedly increased in LPS-stimulated cells compared to that in untreated cells. As the dose of FJU-C28 administered to LPS-stimulated RAW264.7 macrophages was increased, nuclear NF-κB (p65) was decreased; conversely, NF-κB (p65) accumulated in the cytosolic extract (Figure 6C). This result indicated that FJU-C28 could suppress NF-κB transcriptional activity by blocking LPS-induced NF-κB translocation from the cytosol to the nucleus in a concentration-dependent manner.

3.6 | Effects of FJU-C28 on IL-6/STAT3 signaling

To investigate the suppressive effect of FJU-C28 on IL-6/STAT3 signaling in LPS-induced macrophage inflammation, LPS-stimulated cells were treated with FJU-C28 or various MAPK inhibitors, and cell lysates were analyzed by western blot. The results showed that FJU-C28 concentration-dependently inhibited the phosphorylation of STAT3 in LPS-induced RAW264.7 macrophages. In addition, MAPK inhibitors, including SB203580 (p38 MAPK inhibitor) and SP600125 (JNK inhibitor), inhibited the LPS-induced phosphorylation of STAT3 in RAW264.7 macrophages, but PD98059 (ERK inhibitor) slightly suppressed STAT3 phosphorylation. Taken together, these findings show that FJU-C28 plays an important role in suppressing the LPS-induced activation of IL-6/STAT3 signaling by suppressing the activation of JNK and p38 MAPK which mediates the LPS-induced expression of IL-6 in RAW264.7 macrophages (Figure 6D). In addition, the suppressive effect of SP600125 was better than SB203580 because SP600125 also contributed to the inhibitory effect on the phosphorylation of STAT3 induced by IL-6 stimulation (Figure S1). Interestingly, FJU-C28 can dramatically suppress the IL-6/STAT3 signaling induced by LPS through not only inactivating p38 MAPK and JNK but also reducing the levels of STAT3 protein (Figure S2). The proposed mechanism of action regarding FJU-C28 suppressing the IL-6/STAT3 was illustrated in Figure S3.

3.7 | Effect of FJU-C28 on lung function in mice with LPS-induced systemic inflammation

To evaluate the protective effect of FJU-C28 on lung function in mice with systemic inflammation induced by endotoxin, male C57BL/6 mice were administered LPS (7.5 mg/kg) and treated with/without FJU-C28 (5 mg/kg) for 24 h; subsequently, lung function parameters were measured using a Buxco pulmonary function test system. The results showed that compared with normal control mice, mice with LPS-induced systemic inflammation had significantly decreased lung IC, VC, lung compliance (C chord), FEV100, and FVC. However, treatment with FJU-C28 restored the LPS-induced decreases in lung function including VC ($p < .05$), C chord, FEV100 ($p < .05$), and FVC ($p < .05$), compared to those of LPS-treated mice (Figure 7). To confirm the status of LPS-induced lung injury in mice, histological examination of lung specimens was performed by H&E staining. The results demonstrated that neutrophils infiltrated and accumulated in the interstitium of the lungs, and the alveolar

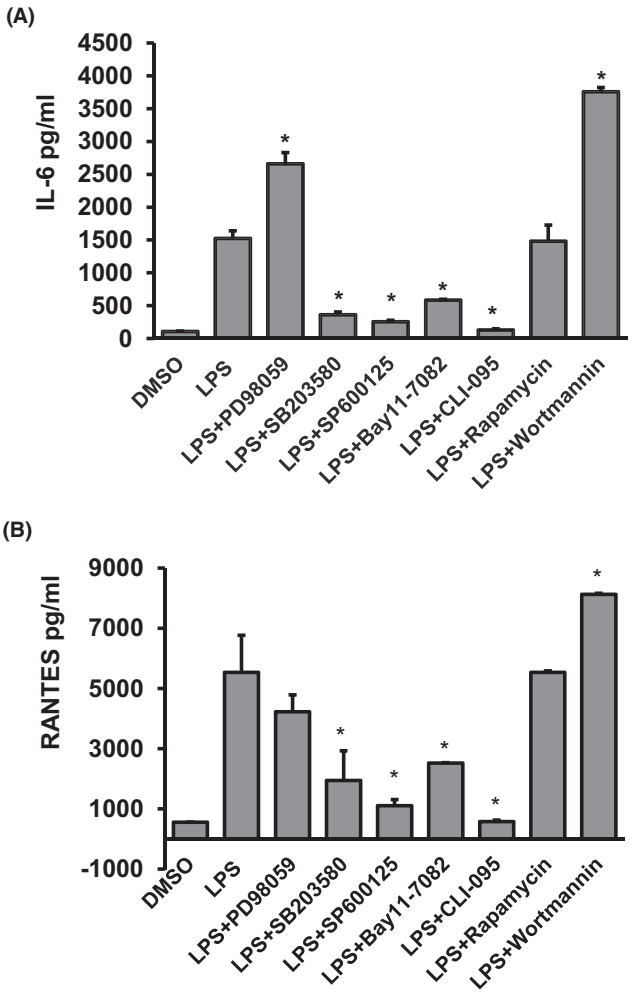

FIGURE 5 The LPS-induced secretion of IL-6 and RANTES were mediated by various signaling pathways. (A) The level of secreted IL-6 and (B) RANTES in conditioned media. RAW264.7 macrophages were pretreated with 10 μM PD98059 (ERK inhibitor), 10 μM SB203580 (p38 MAPK inhibitor), 10 μM SP600125 (JNK inhibitor), 10 μM BAY11-7082 (IkB-α Inhibitor), 1 μg/ml CLI-095 (TLR4 inhibitor), 1 μg/ml Rapamycin (mTOR inhibitor), and 1 μM Wortmannin (PI3-kinase Inhibitor) for 30 min and then stimulated with LPS (100 ng/ml) for 24 h. The conditioned media was harvested and analyzed by ELISA. The quantitative data are expressed as the mean ± *SE* ($n = 2$) $^*p < .05$ compared with LPS treatment. LPS, lipopolysaccharide

structure was destroyed and became thickened and irregular in mice in the LPS stimulation group compared to mice in the control group. Treatment with FJU-C28 reduced the neutrophil infiltration in the interstitium and sustained most of the alveolar structure in mouse lung tissue in the LPS+FJU-C28 treatment group compared to the LPS stimulation group (Figure 8A). To ascertain the correlation between target cytokines and lung injury, serum cytokines were measured by ELISA. The results showed that the circulating levels of IL-6 and RANTES were significantly elevated in mice with LPS-induced systemic inflammation compared to control mice. The secretion of RANTES and IL-6 was significantly suppressed by FJU-C28 treatment (Figure 6C). This finding indicated that FJU-C28 could attenuate lung injury by suppressing the secretion of proinflammatory cytokines, including IL-6 and RANTES, in LPS-induced systemic inflammation.

4 | DISCUSSION

Proinflammatory cytokines are important in cell signaling and promote systemic inflammation; cytokines are predominantly produced by activated macrophages and are involved in the upregulation of inflammatory reactions.[35,36] Proinflammatory cytokines, such as TNFα and IL-6, modulate cell signaling and promote systemic inflammation.[14,37] Recently, alternative anti-inflammatory medicinal compound pirfenidone, a pyridone-related compound, was reported to inhibit the production of TNFα in vitro and in vivo and to prevent septic shock and subsequent mortality.[38] Other pyridone derivatives, 5-ethyl-1-phenyl-2-(1H) pyridine and fluorofenidone (AKF-PD), have been shown to protect mice from lethal endotoxemia induced by LPS stimulation and reduce IL-1, IL-6 and TNFα production.[39,40] In this study, we demonstrated that the newly synthesized pyridine-related compound FJU-C28 could significantly reduce the LPS-induced expression of RANTES and IL-6 (Figure 3). These findings also indicated that the effect of FJU-C28 on LPS-induced inflammatory responses is different from the previously tested compound FJU-C4, in endotoxin-induced inflammation of macrophages.[13]

Cumulative evidence has demonstrated that FJU-C28 is potentially advantageous for preventing inflammatory diseases by inhibiting the NF-κB and MAPK pathways. MAPKs and NF-κB play important roles in mediating extracellular signal transduction to the nucleus and activate the expression of inflammatory cytokines and mediators.[41,42] These results support our findings that FJU-C28 may significantly suppress the expression of the proinflammatory cytokine IL-6 and the activation of STAT3 by regulating the NF-κB, p38 MAPK and JNK signaling pathways. NF-κB is an inactive form that is stabilized by the inhibitory protein IκBα in the cytoplasm and is activated in response to several stimuli, such as proinflammatory cytokines, infections, and physical stress.[43,44] Activated NF-κB translocates from the cytoplasm to the nucleus and regulates the expression of proinflammatory and antiapoptotic genes.[17] This pathway can also be amplified due to the inflammatory response by a positive NF-κB autoregulatory loop and increase the duration of chronic inflammation.[45]

TNFα and IL-6 secretion, as well as neutrophil accumulation and protein leakage in the lungs of mice, was found to be dependent on p38 MAPK signaling.[18] p38 MAPK is activated by a wide range of substrates, and the downstream activities attributed to these phosphorylation events are frequently cell type-specific, including inflammatory responses, cell differentiation, apoptosis, cytokine production and RNA splicing regulation.[46] STAT3 phosphorylation is activated by MAPK, and these pathways play regulatory roles in the production of proinflammatory cytokines and downstream signaling events, leading to the synthesis of inflammatory mediators at the transcriptional and translational levels.[47,48]

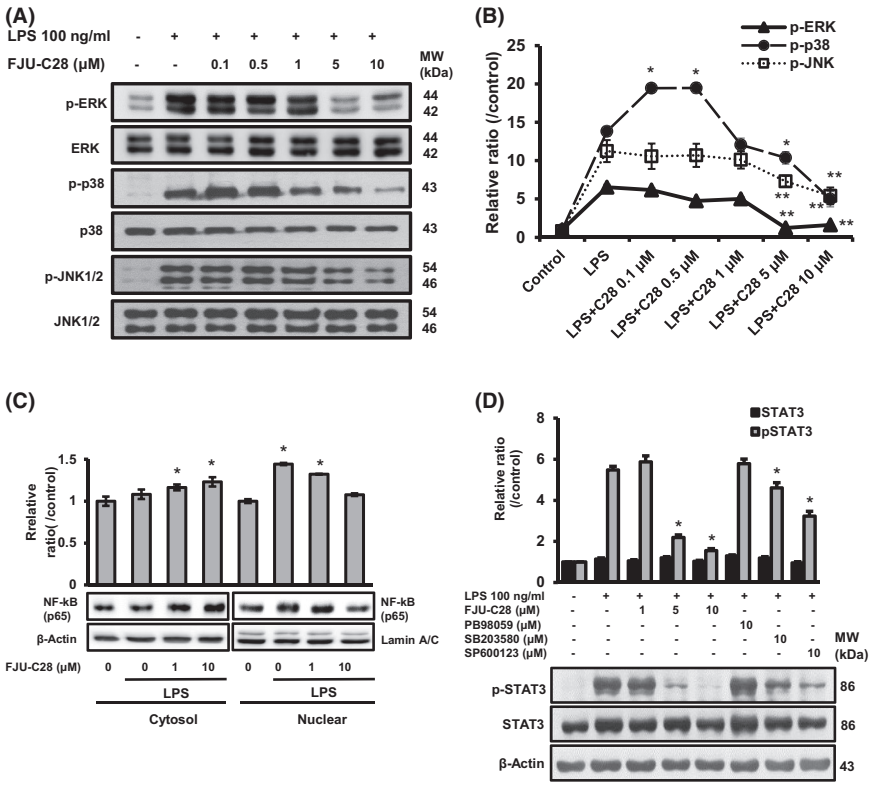

FIGURE 6 Effect of FJU-C28 on the LPS-induced phosphorylation of MAP kinases and NF-κB translocation. (A) Cells were pretreated with 0 to 10 μM FJU-C28 for 30 min, and then the cells were exposed to LPS (100 ng/ml) for 15 min. Cells were harvested and analyzed by western blotting with specific antibodies against MAPK proteins as indicated. (B) The intensity of phosphorylated proteins in the immunoblot was normalized to that of the total protein and is expressed as the relative ratio of the treatment group to the control. The data represent the mean ± *SE* ($n = 3$). (C) Cells were pretreated with FJU-C28 and then were exposed to LPS (100 ng/ml) for 30 min, and the cytoplasmic and nuclear protein fractions were extracted for western blot analysis with anti-NF-κB p65 antibodies. β-Actin and Lamin A/C were used as internal controls. (D) Cells were pretreated with FJU-C28 and MAPK inhibitors as indicated for 30 min, and then the cells were exposed to LPS for 24 h. Cells were harvested and analyzed by western blotting with specific antibodies against p-STAT3 (Tyr705) and STAT3. The data represent the mean ± *SE* ($n = 3$). The quantitative immunoblot data are shown in the upper panel. $^{*}p < .05$ and $^{**}p < .01$ compared with LPS treatment. LPS, lipopolysaccharide; MAPK, mitogen-activated protein kinase; NF-κB, nuclear factor-κB

Successfully suppressing IL-6 and inhibiting the activities of NF-κB and ERK, JNK, and p38 MAPK may have potential therapeutic value in inflammatory-mediated diseases, including the acute-phase response, chronic inflammation, autoimmunity, endothelial cell dysfunction and fibrogenesis.[49,50]

It is interesting why LPS-induced expression of IL-6 is not completely suppressed by SB203580 or SP600125 even at 10 μM, respectively. We propose that LPS can activate NF-κB, p38 MAPK, and JNK signaling pathways to induce the expression of proinflammatory cytokines such as IL-6. SB203580 or SP600125 alone does not completely suppress the expression of IL-6 because other pathways such as NF-κB may drive the production. Therefore, the part of IL-6 cytokines is secreted to their surrounding environment and then binds to membrane-bound IL-6R to activate IL-6/STAT3 signaling and drive the production of IL-6 via an autocrine. In addition, our data also showed that SP600125 but not SB203580 can suppress the phosphorylation of STAT3 induced by IL-6 stimulation. Thus, it indicates that the suppressive effect of SP600125 with two hit points on the activation of STAT3 signaling is better than SB203580 with one hit point as shown in Figure 6D. Based on our current data, we propose that acute exposure to LPS can activate NF-κB, p38 MAPK, and JNK signaling pathways to induce the expression of proinflammatory cytokines such as IL-6 and CCL5. The LPS-induced IL-6 can be secreted to the extracellular environment and then bind to membrane-bound IL-6R to induce IL-6/STAT3 signaling (autocrine) to sustain the production of IL-6 potentially modulating the severity of the host inflammatory response. LPS-induced production of IL-6 is suppressed by FJU-C28 through inhibiting the activation of NF-κB, p38 MAPK and JNK signal pathways; and the activity of IL-6/STAT3 signaling also is inhibited via reducing the levels of STAT3 protein. It is suggested that the reduced levels of STAT3 protein may due to protein degradation. However, these data suggest that the synthetic compound FJU-C28 is a potential inflammatory therapeutic agent for inflammatory-mediated diseases mediated by IL-6/STAT3 signaling, including asthma and inflammatory lung diseases.[9,34,51]

The question regarding whether FJU-C28 could inhibit JAK1/2 and TYK2 kinases is worthy of investigation. Recent references have demonstrated that unsubstituted 2-pyridones can potentially serve as both a H-bond donor and an acceptor

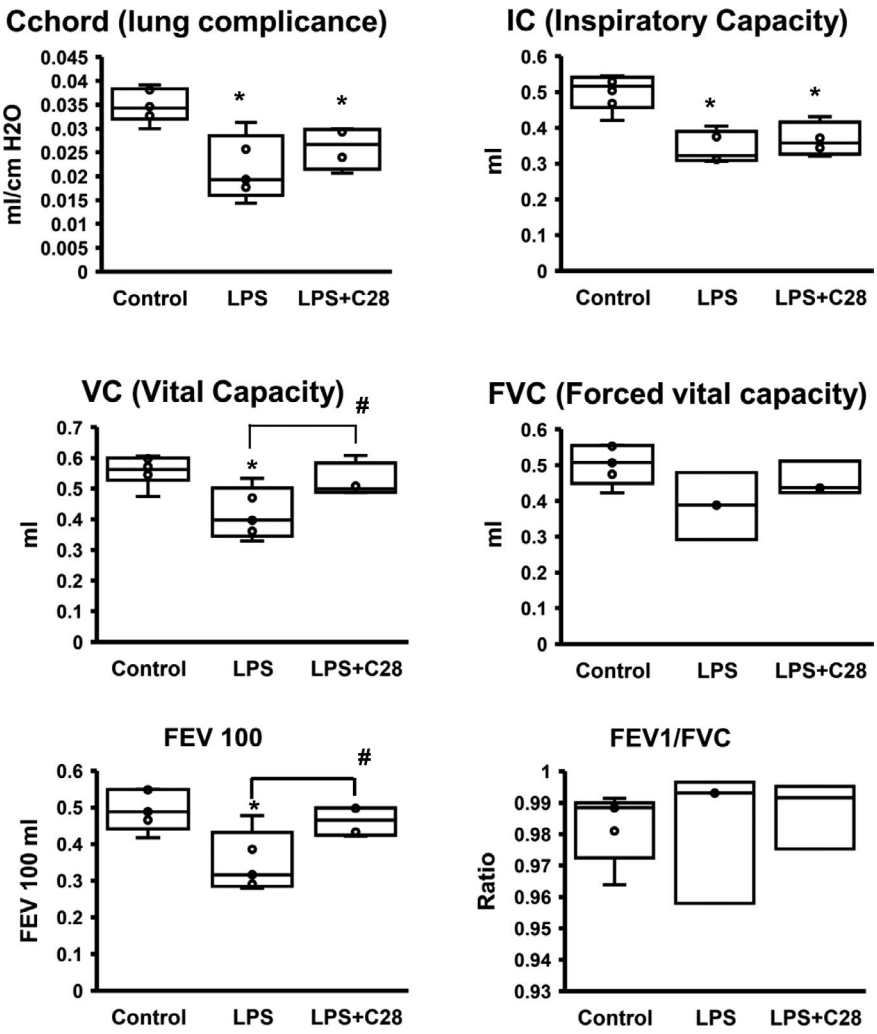

FIGURE 7 Effect of FJU-C28 on preventing endotoxin-induced lung function decrease in mice with systemic inflammation. Male C57BL/6 mice were pretreated with/without FJU-C28 for 30 min and then administered LPS (7.5 mg/kg) for 24 h. Anesthetized mice were endotracheally intubated with an airway catheter, and lung function parameters, namely, IC (inspiratory capacity), VC (vital capacity), C chord (lung compliance), FEV100 (forced expiratory volume at 100 ms), and FVC (forced vital capacity), were measured. The quantitative data are expressed as the mean ± *SE*. Light spots represent the lung function of control mice ($n = 5$). Gray and dark spots represent the lung function of mice with LPS-induced lung injury ($n = 5$) and LPS plus FJU-C28 treatment ($n = 5$), respectively. $^{*}p < .05$ compared with control mice. $^{\#}p < .05$ compared with LPS stimulation alone. LPS, lipopolysaccharide

to inhibit various kinase via interacting with hinge binding scaffolds of kinase protein.[52] Thompson et al. demonstrated that the tetracyclic pyridone contributed the highly selective inhibition to the JAK family members over other kinases such as MEK and IKK2 through interacting between the amide moiety of the pyridone and the backbone Glu and Leu residues in the kinase hinge region.[53] Merck reported that the modified compounds containing 2-pyridone moiety preserving the two H-bond interactions between the amide group and the kinase hinge can significantly improve the inhibitory potency to JAK1 kinase.[54] Cumulative references imply that FJU-C28 with a 2-pyridone moiety may provide kinase inhibition due to its two H-bonds, a donor and an acceptor, as kinase hinge binder to interact with the backbone amino acid residues in the kinase hinge region. Therefore, we observed that several signaling pathways including NF-κB, MAPKs, and IL-6/STAT3 were suppressed by FJU-C28. However, the IC_{50} of individual kinase and the specificity to various kinases will be explored in the future.

AMP-activated protein kinase (AMPK), a regulator of energy metabolism and autophagy, mediates energy homeostasis, including carbohydrate, lipid and protein metabolism. Recent studies have demonstrated that suppressing the activation of AMPK enhances LPS-induced inflammatory responses, including worsening the severity of ALI[55]; conversely, reactivating AMPK exerts potent anti-inflammatory effects and attenuates LPS-induced ALI in vitro and in vivo.[56–58] Zhao et al. showed that RANTES/CCL5 activates autophagy through the AMPK pathway, and autophagy increases migration, which was confirmed by experiments with AMPK inhibitors.[59] Our current study demonstrated that the secretion of IL-6 and RANTES was upregulated in the context of LPS-induced inflammation in vitro and in vivo. The current data suggest that RANTES may be involved in a proinflammatory response associated with hypercatabolism in patients with ALI and ARDS. This finding suggested that IL-6 and RANTES could play important roles in energy metabolism in mice suffering from systemic inflammatory responses. In this study, we found that FJU-C28 was a highly potent compound that blocked the secretion of IL-6 and RANTES in LPS-activated macrophages and mice with endotoxemia. The animal study also showed that treatment with FJU-C28 abrogated the LPS-induced decrease in lung function including VC, lung compliance and FVC. This evidence strongly suggests that FJU-C28 is a highly promising therapeutic agent for the treatment of inflammatory lung injury that ameliorates declines in lung function due to virus-induced or endotoxin-induced

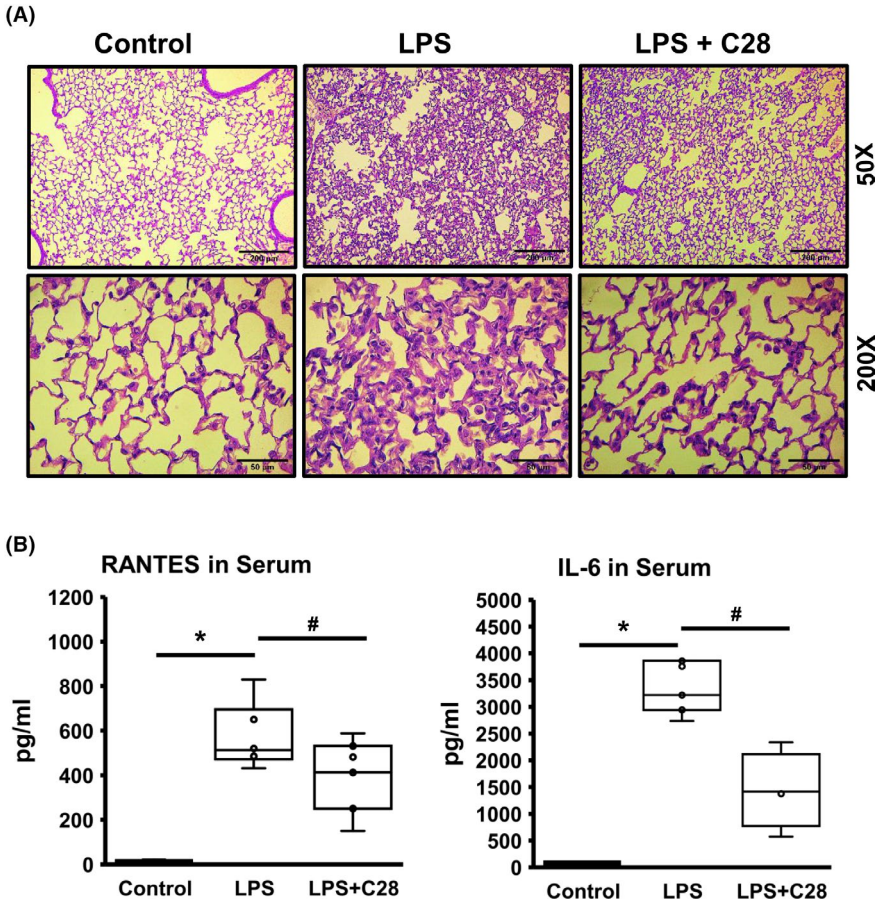

FIGURE 8 FJU-C28 reduced lung damage and circulating levels of IL-6 and RANTES in mice with systemic inflammation. (A) Hematoxylin and eosin staining of lung specimens from control mice (left), LPS-induced mice (middle) and LPS plus FJU-C28-treated mice (right). The photos in the upper panel are at 50× magnification, and those in the lower panel are at 200× magnification. Bar = 100 μm at 50× magnification and 25 μm at 200× magnification as indicated. (B) Cytokines, including RANTES and IL-6, in mouse serum in the control ($n = 6$), LPS ($n = 6$) and LPS plus FJU-C28 treatment ($n = 6$) groups were measured by ELISA. The quantitative data are expressed as means ± *SE*. $^{*}p < .05$ compared with control mice. $^{\#}p < .05$ compared with LPS stimulation alone. LPS, lipopolysaccharide

systemic inflammatory responses by mediating RANTES and IL-6/STAT3 signaling.

5 | CONCLUSION

These findings suggest that FJU-C28 possesses anti-inflammatory activities to prevent endotoxin-induced lung function decrease and lung damages by down-regulating proinflammatory cytokines including IL-6 and RANTES via suppressing the JNK, p38 MAPK, and NF-κB signaling pathways. These results provide additional insight into the mechanism and new opportunities for therapeutic intervention against lung inflammatory disease.

ACKNOWLEDGMENTS

The authors thank Ms. Ming-Lu Wang (School of Medicine, Fu-Jen Catholic University, and Taipei City, Taiwan) and Ms. Tsai-Ni Huang (Department of Respiratory Therapy, Fu-Jen Catholic University) for performing part of the experiments.

AUTHOR CONTRIBUTIONS

FJ carried out the cell-based and animal studies and performed data analysis. JS participated in the design of the study and the data analysis. SH and HY carried out the animal studies. SS helped synthesize the experimental compound. JC participated in the design of the study, performed the western blot analysis, and drafted the manuscript. GM participated in the design of the study and drafted the manuscript. All authors read and approved the final manuscript.

DISCLOSURE

The authors declare that there is no conflict of interest regarding the publication of this paper.

ETHICS APPROVAL

All procedures on animals were approved by the ethics committee of Fu-Jen Catholic University and performed in accordance with institutional animal care guidelines.

DATA AVAILABILITY STATEMENT

All data generated and analyzed during the study are included in the published article and can be shared upon request.

ORCID

Jau-Chen Lin https://orcid.org/0000-0002-4358-0602

REFERENCES

1. Matthay MA, Zemans RL, Zimmerman GA, et al. Acute respiratory distress syndrome. *Nat Rev Dis Primers*. 2019;5(1):18.
2. Shah RD, Wunderink RG. Viral pneumonia and acute respiratory distress syndrome. *Clin Chest Med*. 2017;38(1):113-125.

3. Brown KL, Cosseau C, Gardy JL, Hancock RE. Complexities of targeting innate immunity to treat infection. *Trends Immunol*. 2007;28(6):260-266.
4. Lawrence T, Willoughby DA, Gilroy DW. Anti-inflammatory lipid mediators and insights into the resolution of inflammation. *Nat Rev Immunol*. 2002;2(10):787-795.
5. Zhang X, Mosser DM. Macrophage activation by endogenous danger signals. *J Pathol*. 2008;214(2):161-178.
6. Akarasereenont P, Bakhle YS, Thiemermann C, Vane JR. Cytokine-mediated induction of cyclo-oxygenase-2 by activation of tyrosine kinase in bovine endothelial cells stimulated by bacterial lipopolysaccharide. *Br J Pharmacol*. 1995;115(3):401-408.
7. Kotas ME, Medzhitov R. Homeostasis, inflammation, and disease susceptibility. *Cell*. 2015;160(5):816-827.
8. Peters MC, McGrath KW, Hawkins GA, et al. Plasma interleukin-6 concentrations, metabolic dysfunction, and asthma severity: a cross-sectional analysis of two cohorts. *Lancet Respir Med*. 2016;4(7):574-584.
9. Rincon M, Irvin CG. Role of IL-6 in asthma and other inflammatory pulmonary diseases. *Int J Biol Sci*. 2012;8(9):1281-1290.
10. Fattori E, Cappelletti M, Costa P, et al. Defective inflammatory response in interleukin 6-deficient mice. *J Exp Med*. 1994;180(4):1243-1250.
11. Scheller J, Chalaris A, Schmidt-Arras D, Rose-John S. The pro- and anti-inflammatory properties of the cytokine interleukin-6. *Biochem Biophys Acta*. 2011;1813(5):878-888.
12. Kaplanski G, Marin V, Montero-Julian F, Mantovani A, Farnarier C. IL-6: a regulator of the transition from neutrophil to monocyte recruitment during inflammation. *Trends Immunol*. 2003;24(1):25-29.
13. Liu JS, Jung F, Yang SH, et al. FJU-C4, a new 2-pyridone compound, attenuates lipopolysaccharide-induced systemic inflammation via p38MAPK and NF-kappaB in mice. *PLoS One*. 2013;8(12):e82877.
14. Kwon DJ, Ju SM, Youn GS, Choi SY, Park J. Suppression of iNOS and COX-2 expression by flavokawain A via blockade of NF-kappaB and AP-1 activation in RAW 264.7 macrophages. *Food Chem Toxicol*. 2013;58:479-486.
15. Zhang X, Liu F, Liu H, et al. Urinary trypsin inhibitor attenuates lipopolysaccharide-induced acute lung injury by blocking the activation of p38 mitogen-activated protein kinase. *Inflamm Res*. 2011;60(6):569-575.
16. Sio SW, Ang SF, Lu J, Moochhala S, Bhatia M. Substance P upregulates cyclooxygenase-2 and prostaglandin E metabolite by activating ERK1/2 and NF-kappaB in a mouse model of burn-induced remote acute lung injury. *J Immunol*. 2010;185(10):6265-6276.
17. Lawrence T. The nuclear factor NF-kappaB pathway in inflammation. *Cold Spring Harb Perspect Biol*. 2009;1(6):a001651.
18. Schnyder-Candrian S, Quesniaux VF, Di Padova F, et al. Dual effects of p38 MAPK on TNF-dependent bronchoconstriction and TNF-independent neutrophil recruitment in lipopolysaccharide-induced acute respiratory distress syndrome. *J Immunol*. 2005;175(1):262-269.
19. Craig R, Larkin A, Mingo AM, et al. p38 MAPK and NF-kappa B collaborate to induce interleukin-6 gene expression and release. Evidence for a cytoprotective autocrine signaling pathway in a cardiac myocyte model system. *J Biol Chem*. 2000;275(31):23814-23824.
20. Schall TJ, Bacon K, Toy KJ, Goeddel DV. Selective attraction of monocytes and T lymphocytes of the memory phenotype by cytokine RANTES. *Nature*. 1990;347(6294):669-671.
21. Lee YR, Su CY, Chow NH, et al. Dengue viruses can infect human primary lung epithelia as well as lung carcinoma cells, and can also induce the secretion of IL-6 and RANTES. *Virus Res*. 2007;126(1–2):216-225.
22. Teran LM, Seminario MC, Shute JK, et al. RANTES, macrophage-inhibitory protein 1alpha, and the eosinophil product major basic protein are released into upper respiratory secretions during virus-induced asthma exacerbations in children. *J Infect Dis*. 1999;179(3):677-681.
23. Saito T, Deskin RW, Casola A, et al. Respiratory syncytial virus induces selective production of the chemokine RANTES by upper airway epithelial cells. *J Infect Dis*. 1997;175(3):497-504.
24. Matsukura S, Kokubu F, Kubo H, et al. Expression of RANTES by normal airway epithelial cells after influenza virus A infection. *Am J Respir Cell Mol Biol*. 1998;18(2):255-264.
25. Okabayashi T, Kariwa H, Yokota S, et al. Cytokine regulation in SARS coronavirus infection compared to other respiratory virus infections. *J Med Virol*. 2006;78(4):417-424.
26. Tekkanat KK, Maassab H, Miller A, Berlin AA, Kunkel SL, Lukacs NW. RANTES (CCL5) production during primary respiratory syncytial virus infection exacerbates airway disease. *Eur J Immunol*. 2002;32(11):3276-3284.
27. Dorfmuller P, Zarka V, Durand-Gasselin I, et al. Chemokine RANTES in severe pulmonary arterial hypertension. *Am J Respir Crit Care Med*. 2002;165(4):534-539.
28. Chen CH, Chen YL, Sung PH, et al. Effective protection against acute respiratory distress syndrome/sepsis injury by combined adipose-derived mesenchymal stem cells and preactivated disaggregated platelets. *Oncotarget*. 2017;8(47):82415-82429.
29. Gerard C, Frossard JL, Bhatia M, et al. Targeted disruption of the beta-chemokine receptor CCR1 protects against pancreatitis-associated lung injury. *J Clin Investig*. 1997;100(8):2022-2027.
30. Bhatia M, Proudfoot AE, Wells TN, Christmas S, Neoptolemos JP, Slavin J. Treatment with Met-RANTES reduces lung injury in caerulein-induced pancreatitis. *Br J Surg*. 2003;90(6):698-704.
31. Russkamp NF, Ruemmler R, Roewe J, Moore BB, Ward PA, Bosmann M. Experimental design of complement component 5a-induced acute lung injury (C5a-ALI): a role of CC-chemokine receptor type 5 during immune activation by anaphylatoxin. *FASEB J*. 2015;29(9):3762-3772.
32. Li Q, Mitscher LA, Shen LL. The 2-pyridone antibacterial agents: bacterial topoisomerase inhibitors. *Med Res Rev*. 2000;20(4):231-293.
33. Chou ST, Jung F, Yang SH, Chou HL, Jow GM, Lin JC. Antofine suppresses endotoxin-induced inflammation and metabolic disorder via AMP-activated protein kinase. *Pharmacol Res Perspect*. 2017;5(4):e00337.
34. Shieh JM, Tseng HY, Jung F, Yang SH, Lin JC. Elevation of IL-6 and IL-33 levels in serum associated with lung fibrosis and skeletal muscle wasting in a bleomycin-induced lung injury mouse model. *Mediators Inflamm*. 2019;2019:7947596.
35. Kim KJ, Yoon KY, Yoon HS, Oh SR, Lee BY. Brazilein suppresses inflammation through inactivation of IRAK4-NF-kappaB pathway in LPS-induced Raw264.7 macrophage cells. *Int J Mol Sci*. 2015;16(11):27589-27598.
36. Chao WW, Hong YH, Chen ML, Lin BF. Inhibitory effects of *Angelica sinensis* ethyl acetate extract and major compounds on NF-kappaB trans-activation activity and LPS-induced inflammation. *J Ethnopharmacol*. 2010;129(2):244-249.
37. Aderem A, Ulevitch RJ. Toll-like receptors in the induction of the innate immune response. *Nature*. 2000;406(6797):782-787.
38. Cain WC, Stuart RW, Lefkowitz DL, Starnes JD, Margolin S, Lefkowitz SS. Inhibition of tumor necrosis factor and subsequent endotoxin shock by pirfenidone. *Int J Immunopharmacol*. 1998;20(12):685-695.
39. Tang Y, Li B, Wang N, et al. Fluorofenidone protects mice from lethal endotoxemia through the inhibition of TNF-alpha and IL-1beta release. *Int Immunopharmacol*. 2010;10(5):580-583.
40. Grattendick KJ, Nakashima JM, Giri SN. Effects of 5-ethyl-1-phenyl-2-(1H) pyridone on serum biomarkers of multiorgan dysfunction and mortality in lipopolysaccharide/glactosamine and cecal ligation and puncture models of septic shock in mice. *Res Commun Mol Pathol Pharmacol*. 2009;122–123(1–6):27-50.

41. Lee HS, Ryu DS, Lee GS, Lee DS. Anti-inflammatory effects of dichloromethane fraction from *Orostachys japonicus* in RAW 264.7 cells: suppression of NF-kappaB activation and MAPK signaling. *J Ethnopharmacol*. 2012;140(2):271-276.
42. Kefaloyianni E, Gaitanaki C, Beis I. ERK1/2 and p38-MAPK signalling pathways, through MSK1, are involved in NF-kappaB transactivation during oxidative stress in skeletal myoblasts. *Cell Signal*. 2006;18(12):2238-2251.
43. Hoesel B, Schmid JA. The complexity of NF-kappaB signaling in inflammation and cancer. *Mol Cancer*. 2013;12:86.
44. Yamamoto Y, Gaynor RB. Therapeutic potential of inhibition of the NF-kappaB pathway in the treatment of inflammation and cancer. *J Clin Investig*. 2001;107(2):135-142.
45. Pahl HL. Activators and target genes of Rel/NF-kappaB transcription factors. *Oncogene*. 1999;18(49):6853-6866.
46. Coulthard LR, White DE, Jones DL, McDermott MF, Burchill SA. p38(MAPK): stress responses from molecular mechanisms to therapeutics. *Trends Mol Med*. 2009;15(8):369-379.
47. Kim EK, Choi EJ. Pathological roles of MAPK signaling pathways in human diseases. *Biochem Biophys Acta*. 2010;1802(4):396-405.
48. Han J, Lee JD, Bibbs L, Ulevitch RJ. A MAP kinase targeted by endotoxin and hyperosmolarity in mammalian cells. *Science*. 1994;265(5173):808-811.
49. Reeves MB, Compton T. Inhibition of inflammatory interleukin-6 activity via extracellular signal-regulated kinase-mitogen-activated protein kinase signaling antagonizes human cytomegalovirus reactivation from dendritic cells. *J Virol*. 2011;85(23):12750-12758.
50. Kim JY, Bae YH, Bae MK, et al. Visfatin through STAT3 activation enhances IL-6 expression that promotes endothelial angiogenesis. *Biochem Biophys Acta*. 2009;1793(11):1759-1767.
51. Park WY, Goodman RB, Steinberg KP, et al. Cytokine balance in the lungs of patients with acute respiratory distress syndrome. *Am J Respir Crit Care Med*. 2001;164(10 pt 1):1896-1903.
52. Zhang Y, Pike A. Pyridones in drug discovery: recent advances. *Bioorg Med Chem Lett*. 2021;38:127849.
53. Thompson JE, Cubbon RM, Cummings RT, et al. Photochemical preparation of a pyridone containing tetracycle: a Jak protein kinase inhibitor. *Bioorg Med Chem Lett*. 2002;12(8):1219-1223.
54. Simov V, Deshmukh SV, Dinsmore CJ, et al. Structure-based design and development of (benz)imidazole pyridones as JAK1-selective kinase inhibitors. *Bioorg Med Chem Lett*. 2016;26(7):1803-1808.
55. Park DW, Jiang S, Liu Y, et al. GSK3beta-dependent inhibition of AMPK potentiates activation of neutrophils and macrophages and enhances severity of acute lung injury. *Am J Physiol Lung Cell Mol Physiol*. 2014;307(10):L735-L745.
56. Chen L, Li W, Qi D, Lu L, Zhang Z, Wang D. Honokiol protects pulmonary microvascular endothelial barrier against lipopolysaccharide-induced ARDS partially via the Sirt3/AMPK signaling axis. *Life Sci*. 2018;210:86-95.
57. Park DW, Jiang S, Tadie JM, et al. Activation of AMPK enhances neutrophil chemotaxis and bacterial killing. *Mol Med*. 2013;19:387-398.
58. Jian MY, Alexeyev MF, Wolkowicz PE, Zmijewski JW, Creighton JR. Metformin-stimulated AMPK-alpha1 promotes microvascular repair in acute lung injury. *Am J Physiol Lung Cell Mol Physiol*. 2013;305(11):L844-L855.
59. Zhao H, Chen D, Cao R, et al. Alcohol consumption promotes colorectal carcinoma metastasis via a CCL5-induced and AMPK-pathway-mediated activation of autophagy. *Sci Rep*. 2018;8(1):8640.

SUPPORTING INFORMATION

Additional Supporting Information may be found in the online version of the article at the publisher's website.

How to cite this article: Jung F, Liu J-S, Yang S-H, et al. FJU-C28 inhibits the endotoxin-induced pro-inflammatory cytokines expression via suppressing JNK, p38 MAPK and NF-κB signaling pathways. *Pharmacol Res Perspect*. 2021;9:e00876. doi:10.1002/prp2.876